**Atmospheric
Chemistry
and Physics
Discussions**

Single particle characterization of black carbon aerosol in the Northeast Tibetan Plateau, China

Q. Y. Wang[1,2], J. P. Schwarz[3,4], J. J. Cao[2,5], R. S. Gao[3], D. W. Fahey[3,4], and T. F. Hu[2]

[1]Department of Environmental Science and Engineering, Xi'an Jiaotong University, Xi'an 710049, China
[2]Key Laboratory of Aerosol, SKLLQG, Institute of Earth Environment, Chinese Academy of Sciences, Xi'an 710075, China
[3]Chemical Sciences Division, Earth System Research Laboratory, NOAA, Boulder, Colorado, USA
[4]Cooperative Institute for Research in Environmental Sciences, University of Colorado, Boulder, Colorado USA
[5]Institute of Global Environmental Change, Xi'an Jiaotong University, Xi'an 710049, China

Correspondence to: J. J. Cao (cao@loess.llqg.ac.cn)

Abstract

Refractory black carbon (rBC) mass, size distribution, and mixing state were measured with a ground-based Single Particle Soot Photometer (SP2) at Qinghai Lake (QHL), a rural area in the Northeastern Tibetan Plateau of China, during October 2011. The average measured rBC mass concentration of $0.36\,\mu g\,STP\text{-}m^{-3}$ is significantly higher than the concentrations measured in background and remote regions around the globe. The diurnal variation of rBC concentration showed nocturnal peak and afternoon low concentrations and showed a loose anticorrelation to the variation of mixed layer depths, indicating nighttime trapping of emissions and daytime ventilation. The high rBC values and their diurnal behavior strongly suggest that the QHL area was heavily influenced by local rBC sources. The mass size distribution of rBC showed a primary mode peak at 175-nm diameter and a small secondary mode peak at 495 nm volume-equivalent diameter assuming $2\,g\,cm^{-3}$ void free density. About 40 % of the observed rBC particles within the detectable size range were mixed with large amounts of non-refractory materials present as a thick coating. A comparison of the Aethalometer and SP2 measurements suggests that there are non-BC species strongly affecting the Aethalometer measurement and, therefore, the Aethalometer measurements are not reliable for rBC determinations in the Tibetan Plateau region without artifact corrections. The apparent black-carbon specific, mass-absorption cross section derived from the Aethalometer and SP2 data was $37.5\,m^2\,g^{-1}$ at a wavelength of 880 nm. A strong correlation was found between rBC and CO with a slope of $1.5 \pm 0.1\,ng\,STP\text{-}m^{-3}\,ppbv^{-1}$, similar to values of mixed rural emissions.

1 Introduction

Black carbon aerosol (BC), a nearly omnipresent byproduct of incomplete combustion, is the most strongly light-absorbing component in the atmosphere and plays a major role in climate change (Jacobson, 2004, 2006). It is considered to be the second or third

largest contributor to anthropogenic radiative forcing after CO_2 (IPCC, 2007). Due to its non-uniform spatio-temporal distribution, BC induces more dramatic regional forcing than either CO_2 or methane (Tripathi et al., 2005; Chung et al., 2005, 2010). For example, BC's global, direct, anthropogenic radiative forcing is estimated to be $\sim 0.34\,\mathrm{W\,m^{-2}}$
5   (Forster et al., 2007), while regional surface forcing in Northern India can reach as high as $62\,\mathrm{W\,m^{-2}}$ (Tripathi et al., 2005). The radiative properties of BC strongly depend on its mixing state. We use the term "BC particle" to refer to any particle containing light-absorbing refractory black carbon (rBC) mass whether or not other non-rBC material is present. When rBC masses are internally mixed with other non-refractory materi-
10   als, their absorption of solar radiation can be enhanced by a factor of about 1.5–2.0 compared to that of externally mixed rBC (Bond et al., 2006; Schnaiter et al., 2005). The mixing state of freshly emitted rBC depends on combustion conditions. As emissions age, rBC becomes more internally mixed through a variety of mechanisms including condensation of emitted gases or those produced in photochemical oxidation
15   processes (Oshima et al., 2009; Petters et al., 2006). In addition to climate forcing, BC particles may have further potential consequences, such as global dimming (Wild et al., 2007), adverse health effects (Pope III and Dockery, 2006), lower crop yields (Chameides et al., 1999), and negative impacts on terrestrial and aquatic ecosystems (Forbes et al., 2006).
20   Numerous studies have examined rural and urban BC in China (e.g. Cao et al., 2003, 2005, 2007; Han et al., 2008). However, there are only limited studies in the Tibetan Plateau (Cao et al., 2009a, 2010; Engling et al., 2011) using filter-based techniques, which measure bulk aerosol absorption rather than rBC mass concentration specifically. Due to the systematic limitations of most of the current filter-based BC measure-
25   ments (Subramanian et al., 2006, 2007), direct examination of the rBC size distribution and mixing state are not possible. Here we report measurements of rBC masses of individual aerosol particles at the shore of Qinghai Lake made with an SP2 instrument.

Qinghai Lake (QHL), the largest closed semi-saline lake in China, is located at 3200 m on a basin on the Northeast Tibetan Plateau (Fig. 1), which is affected by

the East Asian summer monsoon, Indian summer monsoon, winter monsoon, and the westerly jet stream (Xu et al., 2006). The ecological state of QHL has attracted attention worldwide (Lister et al., 1991; Jin et al., 2010).

With high sensitivity and precision, the SP2 provides single particle measurements of rBC mass, size distribution, and mixing state (Schwarz et al., 2006; Gao et al., 2007). The primary objectives of the QHL study were (1) to quantify rBC mass concentrations, size distribution, and mixing state, (2) to derive the rBC mass absorption cross section (MAC) from these observations, and (3) to determine the relationship between rBC and CO to estimate relative emission factors.

2 Experimental methods

Measurements were taken from 16 to 27 October, 2011 on the rooftop (~ 15 m above ground level) of a sampling tower at the "Bird Island" peninsula (36.98° N, 99.88° E), which is located at the northwest section of the QHL shore as shown in Fig. 1. There are four counties around QHL (Fig. 1), including Gangcha, Haiyan, Gonhe, and Tian-jun, with a total population of $\sim 230\,000$. Each day thousands of diesel vehicles pass through the QHL basin via national highways surrounding the lake. Biofuels (e.g. yak dung, sheep fecal pellets, firewood, and crop residues) are the main energy source in rural Qinghai, accounting for $\sim 80\,\%$ of total household energy, of which $\sim 65\,\%$ derives from burning yak dung and sheep fecal pellets (Ping et al., 2011). Trash burning is prevalent in the area.

The operating principles of the SP2 have been described in detail elsewhere (Schwarz et al., 2006). Briefly, the SP2 measures rBC mass in individual rBC-containing particles using intense, intracavity YAG laser light at a wavelength of 1064 nm. When an rBC-containing particle passes through the laser beam, the rBC core is heated to its vaporization temperature and emits incandescent light. The intensity of the incandescence signal is linearly related to the rBC mass and independent of the rBC particle morphology or mixing state over most of the rBC mass range typically

Title Page

Abstract | Introduction

Conclusions | References

Tables | Figures

◄ | ►|

◄ | ►

Back | Close

Full Screen / Esc

Printer-friendly Version

Interactive Discussion

observed in the accumulation mode (Slowik et al., 2007). The instrument detects rBC core sizes in the range of 0.07–1.0 μm volume equivalent diameter (VED), assuming an rBC density of $2\,g\,cm^{-3}$. The incandescence signal was calibrated pre- and post-sampling period using commercially available standard fullerene soot (Lot F12S011,
5 AlphaAesar, Inc., Ward Hill, Massachusetts) provided by the SP2 research group of the NOAA Earth System Research Laboratory. The size of fullerene soot was selected by a differential mobility analyzer (DMA) upstream of the SP2 over a range 125–400 nm mobility diameter, and a linear calibration was extracted from this data.

Monodisperse polystyrene latex spheres (PSL) of different sizes were used to cali-
10 brate the scattering signal. PSL particles (269 nm diameter) were used daily to monitor the laser intensity to ensure the stability of the SP2 during the entire experiment. The uncertainty in the rBC mass determination is ∼ 25 % due to uncertainties in the rBC mass calibration, sample flow measurement, and estimation of rBC mass outside of SP2 detection range. The SP2 sampled air through a cyclone inlet (URG, Chapel Hill,
15 NC), restricting the sizes of ambient particles entering the instrument to below either 1.0-μm or 2.5-μm diameter depending on setup.

The delay time between the peaks in the scattered light signal and the incandescence signal, and the ratio of their intensities (S/I) were used to approximate the amount of non-refractory material coexisting with the rBC mass (loosely referred as
20 rBC coating thickness hereafter) (Schwarz et al., 2006). The delay occurs because the heat generated by the absorption of laser light by rBC cores must evaporate any rBC coating before the onset of rBC incandescence. For an uncoated rBC core, the time delay is small (i.e. less than 2 μs) and S/I is also small (i.e. less than 10). Internally mixed rBC particles are marked by a larger time delay and an increase in the S/I ratio
25 over that of an uncoated rBC particle. This behavior is indicated in Fig. 2, which shows results for more than 1.1×10^4 ambient rBC particles selected from those collected on 16 October during the experiment. Below a 2 μs delay time, the S/I ratio increases smoothly with particle mass over a range of delay times. In contrast, delay times above 2 μs show a strong positive correlation with the S/I ratios, which can increase by more

than an order of magnitude. Thus, 2 μs is used as a proxy to identify the detection threshold of internally mixed rBC particles in this study, which is consistent with that found in Moteki et al. (2007).

An Aethalometer (Model AE-16, Magee Scientific, Berkeley, USA) at a wavelength (λ) of 880 nm was used to measure the attenuation of light transmitted through a quartz-fiber filter that collects particles from a continuous flow of ambient air at 5-min intervals. Mass concentrations of rBC are derived from the light attenuation measurement according to:

$$rBC = \left(1/\sigma_{ATN}\right)\left(A\ln\left(I_1/I_2\right)/Q\right) \tag{1}$$

where I_1 and I_2 are the ratios of the transmitted light intensities for the aerosol-loaded filter at times t_1 and t_2 and for a blank filter respectively; σ_{ATN} is the MAC of rBC aerosol on the filter matrix in $m^2 g^{-1}$; A is area of the filter in m^2 that is exposed to the sample air flow; Q is the amount of sampled air in STP-m^3; and rBC concentration has units of $g\,(STP\text{-}m^3)^{-1}$. STP-m^3 stands for a cubic meter of air at 273.15 K and 1013 hPa. In this study, σ_{ATN} was assumed to be 16.6 $m^2 g^{-1}$, which is the manufacture's default value derived from comparison with thermal elemental carbon measurements. rBC mass concentrations estimated using Eq. (1) will be an upper limit if non-BC aerosol contributes to either the absorption or extinction of the Aethalometer light signal.

Five-minute average mixing ratios of carbon monoxide (CO) gas were obtained using gas-filter correlation technology with infrared photometric detection (Ecotech Model EC9830T Carbon Monoxide Analyzer, Australia) with a detection limit of 20 ppb. Hourly temperature, wind speed, and relative humidity (RH) were obtained from the Gangcha national reference climatological station, ~ 45 km northeast from the sampling site (see Fig. 1). Hourly mixed layer depths (MLDs) during the study period were calculated from the upper-air meteorological data based on the hourly average sounding value archived by the US National Oceanic and Atmospheric Administration (NOAA, http://www.arl.noaa.gov/ready/hysplit4.html).

3 Results and discussion

3.1 rBC mass loading

rBC mixing ratios obtained during the experiment are shown as 5-min averages in Fig. 3, along with other measurements. Statistical values for rBC, CO, and the percent of coated particles are listed in Table 1. rBC varied from 0.05 to 1.56 µg STP-m^{-3}, with an average of 0.36 µg STP-m^{-3}. The average rBC concentration at QHL was a factor of ∼ 17 lower than the value measured with an SP2 at an urban site in Shenzhen, China (Huang et al., 2012), where rBC concentrations varied from 0.42 to 37.0 µg STP-m^{-3}, with an average of 6.0 µg STP-m^{-3}. The average rBC concentration at QHL was also ∼ 10 times lower than the SP2 values obtained at rural sites in the Pearl River Delta (PRD) region of China (3.3–4.1 µg STP-m^{-3}) (Huang et al., 2011, 2012). The large differences are due to the greater emissions of rBC from vehicles and other combustion sources in the PRD region. In comparison with other remote areas in the world, the average rBC concentration at QHL is similar to values found at Fukue Island in Japan (0.32 µg STP-m^{-3}, measured with an SP2, Shiraiwa et al., 2008) where rBC was influenced by Asian outflow, and was 1–2 orders of magnitude higher than values found at the Jungfraujoch alpine site in Switzerland (0.003–0.03 µg STP-m^{-3}, measured with an SP2, Liu et al., 2010). Although BC concentrations estimated using the filter-based method can be enhanced by BC coatings and non-BC aerosol species (Liousse et al., 1993; Coen et al., 2010), the average rBC concentration at QHL is still ∼ 34 % higher than that measured by an Aethalometer in Waliguan (Ma et al., 2003), the highest Global Atmospheric Watch (GAW) station, which is about 130 km southeast from the sampling site (see Fig. 1). Moreover, the average rBC concentration at QHL is considerably higher than values observed in polar areas using Aethalometers (0.001–0.006 µg m^{-3}) (Bodhaine, 1995; Wolff and Cachier, 1998). These comparisons suggest that the values found at the rural QHL site are well above background values and, hence, are very likely influenced by local rBC sources.

Figure 4 shows the diurnal variations of rBC and meteorological conditions averaged overall data available during the experiment period. A clear average diurnal variation in rBC concentrations was observed with minimum values in the late afternoon between 16:00 and 19:00 local standard time (LST) and broad nocturnal maximum values be-tween 00:00 and 03:00 LST. Such nocturnal peak and afternoon low concentrations of rBC are very similar to those observed by an Aethalometer at the southeastern edge of the Tibetan Plateau in China (Engling et al., 2011), as well as those observed at urban sites in Xi'an (Aethalometer) and Shenzhen (SP2), China (Cao et al., 2009b; Huang et al., 2012).

The QHL diurnal cycle is likely due to variations in local meteorological conditions, and is shown averaged over the measurement cycle in Fig. 4. The low average MLDs at night shown in Fig. 4 in the night likely resulted in locally produced pollution be-ing trapped near the surface, leading to high rBC concentrations at night. The MLDs increased after sunrise in response to solar heating, with the induced turbulent dilu-tion leading to a decreasing trend of rBC concentrations during the daytime. A local, slightly higher concentration of rBC appeared in the morning around 08:00 LST, which corresponds to local residential activities (e.g. cooking and heating) in the surrounding villages, although the population near the sampling site was very sparse. In contrast, the morning peak of rBC in Xi'an and Shenzhen showed an obvious BC peak around 08:00–09:00 LST (Cao et al., 2009b; Huang et al., 2012), which was caused by rush hour traffic. The strong diurnal rBC variation shown in Fig. 4 further suggests that the QHL basin is heavily influenced by local rBC sources.

3.2 rBC mass size distribution and mixing state

Figure 5 shows the average size distribution of rBC as a function of volume equiva-lent diameter (assuming a specific density of $2\,\mathrm{g\,cm^{-3}}$) obtained over the entire mea-surement period. A two-mode lognormal function fits the data well between 0.07 and 1.0 μm. The size distribution has a primary mode with a peak at 175 nm, which is within the range of 150–230 nm reported by previous SP2 studies (Huang et al., 2012, and

references therein) assuming the same rBC density of $2\,\mathrm{g\,cm^{-3}}$ for valid comparison. Different emission sources produce BC size distributions with different mode peaks. McMeeking et al. (2010) found an rBC peak diameter of $\sim 165\,\mathrm{nm}$ in the urban plume from Liverpool/Manchester, while the peak in a Texas urban plume was $\sim 170\,\mathrm{nm}$
5 (Schwarz et al., 2008). In addition, the rBC peak diameter in a biomass burning plume in Asian was reported to be $\sim 210\,\mathrm{nm}$ (Kondo et al., 2011), which is also similar to a biomass burning plume in Texas ($\sim 210\,\mathrm{nm}$) (Schwarz et al., 2008). As mentioned above, biofuel burning and diesel vehicles were the main rBC sources at QHL. Thus, the mass diameter peak of 175 nm represents a feature of mixed rBC sources in the
10 QHL region. The secondary mode has a peak at 495 nm, and contains less 10 % of the total rBC mass. Huang et al. (2011) also reported a secondary mode with a peak at 690 nm at a polluted rural location in Kaiping, China, which was 1.4 times higher than the value at QHL.

The number fraction of coated rBC is a useful parameter in defining the extent of
15 internal mixing in an ambient sample. Figure 3 and Table 1 present the time series and statistical values of the number fractions of coated rBC during the sampling period, respectively. We note that the lower coating detection limit was estimated to be equivalent to approximately a 30-nm layer on the rBC mass-equivalent sphere for this campaign (Schwarz et al., 2008). The number fraction of coated rBC ranged from 20–
20 50 %, with an average of 37 %. As shown in Fig. 4, the average diurnal pattern of the number fraction of coated rBC exhibited nearly flat distribution with 7.6 % higher coated fraction during the daytime (38.3 %) than that in the nighttime (35.6 %). The slight enhancement of coated rBC number fraction between 12:00 and 16:00 LST, corresponded to high temperatures but low rBC concentrations. This is a reasonable result
25 considering that strong sunlight can help photochemical oxidation processes that produce condensable material. Variability in this metric was larger during the day than at night, suggesting that nighttime aerosol was less influenced by individual sources for short times. The diurnal variation of the number fractions of coated rBC in Shenzhen also showed a maximum in the afternoon, consistent with this study, but there were

obvious minimum values in the morning and evening, which were both attributed to external mixtures of rBC from strong vehicular emissions during rush hours (Huang et al., 2012).

The relation between rBC concentrations and mixing state was examined. Figure 6 plots number fraction of coated rBC as a function of rBC concentration. Although a weak correlation between the two exists, the structure of the relationship suggests the influence of different sources. High variability in coated fraction exists when rBC concentration levels were $< 0.36\,\mu g\,m^{-3}$, the number fraction of coated rBC was as low as $\sim 20\,\%$ while as high as $\sim 50\,\%$. This large variability is mainly attributable to the local rBC sources, since diesel trucks generally produce rBC with little coating, while biofuel burning produces thickly coated rBC. At higher rBC concentrations ($> 0.40\,\mu g\,m^{-3}$), the number fraction of coated rBC mostly exceeded 37 %. This phenomenon was primarily observed during the night (Fig. 3), which may be attributed to the drop off of diesel traffic in the evenings, combined with the continued contributions of biomass burning for cooking and heating. In contrast, the earlier findings of Huang et al. (2012) at an urban site in Shenzhen showed that extremely high rBC pollution was caused by a complex of comparable contributions from both fresh local emissions and aged particles from regional transport.

3.3 Particle light absorption and rBC

The SP2 does not provide aerosol absorption information. Instead, the rBC loadings measured by the SP2 are compared with BC loadings derived from the Aethalometer absorption measurements to evaluate the potential of Aethalometer artifacts at QHL. Note that the Aethalometer BC values are derived by assuming all absorption in is due to rBC and using a MAC value of 16.6 of $m^2\,g^{-1}$. A linear correlation between BC concentrations derived from the Aethalometer measurements and rBC values from the SP2 is shown in Fig. 7a. The high correlation coefficient of 0.95 implies good measurement consistency. However, the slope of the correlation (2.5) is unusually high.

To further evaluate the Aethalometer, additional measurements were conducted from 27 June to 3 July, 2012, at an urban site on the rooftop (~ 10 m a.g.l.) of the Institute of Earth Environment, Chinese Academy of Sciences (IEECAS; Cao et al., 2009b) in Xi'an, China, using the same SP2 and Aethalometer instruments. Excellent correlation was also found in Xi'an between these same two instruments. However, the correlation slope of 1.3 is much lower than the value obtained at QHL. Lan et al. (2011) also found a similar slope of BC to rBC (1.0) in Shenzhen, another urban area. Since an Aethalometer measures attenuation of light passing through a filter, even non-absorbing particles, such as soil, sulfate, organics, and water, can affect the derived BC value (Hansen et al., 1984). Barring some unknown instrument error, the slope of 2.5 indicates that non-BC aerosol species strongly affect the Aethalometer at QHL. Careful examination and correction of the Aethalometer data are necessary for measurements made in the Tibetan Plateau region (Coen et al., 2010, and references therein). Another possibility is that another absorbing non-rBC species is contributing to the Aethalometer attenuation. Waliguan, China (Ma et al., 2003), the highest Global Atmospheric Watch (GAW) station, is ~ 130 km southeast from the QHL sampling site (see Fig. 1). Aethalometer-measured BC loadings there were consistently lower than these measured at QHL, but since Waliguan is not very far from QHL, BC concentrations there derived from Aethalometers may also need careful examinations and possibly new interpretations.

The MAC value is the most important parameter for deriving BC using an Aethalometer, and the MAC derived from measurements varies with time and location of the measurements (Sharma et al., 2002). Due to the capability of the SP2 to measure the rBC mass directly, the value of MAC can be derived through Eq. (1) using the Aethalometer measured light absorption and the rBC mass concentration assuming that rBC is the only absorbing component in the ambient aerosol. The distribution of the specific MAC values for the BC particles measured during this study is shown in Fig. 7b. A Gaussian mean (and standard deviation) value of $37.5 \pm 0.2\,\mathrm{m^2\,g^{-1}}$ at $\lambda = 880$ nm is obtained at QHL, which is 2.3 times the Aethalometer default value of $16.6\,\mathrm{m^2\,g^{-1}}$.

A range of specific MAC values have been reported by investigations in different regions. Zhang et al. (2008) found MAC varied from 7.3 to 18.0 $m^2 g^{-1}$ at multiple locations in China for an Aethalometer, which was much lower than the value at QHL. MAC values also reached as high as 54.8 and 44.2 $m^2 g^{-1}$ for Aethalometer measurements in Rochester and Philadelphia, USA, respectively (Jeong et al., 2004), which was 13–40 % higher than the value at QHL. The variability of MAC is believed to be associated with emission sources and combustion conditions (Schwarz et al., 2008), and highly influenced by the size, coating, and aging of BC particles (Bond et al., 2006), as well as interferences in quantification of BC using methods that are not specific to rBC (Watson et al., 2005).

3.4 Relationship between black carbon and carbon monoxide

As shown in Fig. 3 and Table 1, the CO mixing ratio varied during the measurement period from 34 to 634 ppb, with an average of 220 ppb. Although the average CO mixing ratio was much lower than observed in Eastern China (Guo et al., 2004; Tu et al., 2007), it was ~ 75 % higher than in nearby Waliguan (126 ppb). Previous studies have indicated that rBC is strongly correlated with CO in urban environments (Baumgardner et al., 2002; Kondo et al., 2006), whereas rBC was less well correlated with CO when farther away from emission sources (Spackman et al., 2008). Figure 8 shows that a relatively tight relationship is found between rBC and CO, with a correlation coefficient of 0.83, indicating that CO was from similar local sources (e.g. yak dung and diesel vehicles) as rBC. Previous studies have pointed out that the emission ratio of rBC to CO was dependent on source type (Bond et al., 2004), so variations in measured ratios could indicate the presence of different sources. For example, urban plumes mostly consist of mobile emissions that are expected to have a low rBC/CO emission ratio, while a high ratio was found in biomass burning plumes (Spackman et al., 2008). As shown in Fig. 8, the derived rBC/CO ratio was 1.54 $ng m^{-3} ppbv^{-1}$. Although high rBC/CO ratios (7–10 $ng m^{-3} ppb^{-1}$, Warneke et al., 2009) were found from biomass burning, there is a lack of research about combustion products from the burning of yak

Single particle characterization of black carbon aerosol

Q. Y. Wang et al.

Title Page

Abstract	Introduction
Conclusions	References
Tables	Figures

|◄ | ►|

◄ | ►

Back | Close

Full Screen / Esc

Printer-friendly Version

Interactive Discussion

dung and sheep fecal pallets. Li et al. (2012) found that 30-s peak values of the CO mixing ratio from yak dung burning can reach as high as ∼ 80 ppm. Kondo et al. (2011) reported rBC/CO ratios from biomass burning were 1.7 and 3.4 during smoldering and flaming phases, respectively. Since yak dung and sheep fecal pallets burning are likely in the smoldering phase (Kang et al., 2009), they likely produce more CO compared to BC leading to the low rBC/CO ratios.

For further perspective, the rBC/CO ratio derived from this study was compared with those SP2 measurements from other studies. McMeeking et al. (2010) measured rBC/CO ratios ranging from 0.8 to 6.2 $\mathrm{ng\,m^{-3}\,ppbv^{-1}}$ in the boundary layer over Europe. Baumgardner et al. (2007) found an rBC/CO ratio of 1.0 $\mathrm{ng\,m^{-3}\,ppbv^{-1}}$ for ground-based measurements in Mexico City, while Subramanian et al. (2010) observed a higher average ratio of 2.9 $\mathrm{ng\,m^{-3}\,ppbv^{-1}}$ over Mexico. Liu et al. (2010) reported an rBC/CO ratio of 1.5 $\mathrm{ng\,m^{-3}\,ppbv^{-1}}$ at Jungfraujoch alpine in Switzerland, which was similar to the ratio at QHL. The diversity of rBC/CO ratios was found between studies, because their emission ratios were highly dependent on the source fuel type, combustion efficiencies, and a possible secondary source of CO from VOC oxidation (Bond et al., 2004; McMeeking et al., 2010), as well as the influence of meteorological conditions (Oshima et al., 2012).

4 Conclusions

An SP2, an Aethalometer, and a CO instrument were deployed at Qinghai Lake in the NE Tibetan Plateau from 16 to 27 October 2011 to characterize the rBC size distribution and mixing state and their relationship to aerosol absorption and CO. The average rBC mass concentration (0.36 $\mathrm{\mu g\,STP\text{-}m^{-3}}$) was significantly higher than that measured in background and remote regions of the globe, indicating that QHL was heavily influenced by local rBC sources. The diurnal rBC variation showed minimum values in the late afternoon and broad nocturnal maximum values, consistent with high mixed-layer depths in the afternoon and low depths in the night. This indicates that local emissions

of rBC are trapped in the QHL basin in the night. The rBC size distribution showed a two-mode lognormal pattern with a primary mode peak at 175 nm, which may represent the features of mixed rBC sources in the QHL region. The small secondary mode with a peak at 495 nm has rarely been measured in previous SP2 observations.

5 The average number fraction of coated rBC was found to be 38 % with daytime values only 7.6 % higher than nighttime values, suggestive of some photochemical oxidation products forming in sunlight. The Aethalometer-SP2 intercomparison suggests that there were non-BC aerosol species affecting the Aethalometer measurements at QHL. The results suggest that Aethalometer measurements are not reliable for rBC

10 determinations in the Tibetan Plateau region without artifact corrections. The apparent specific MAC was $37.5 \, \text{m}^2 \text{g}^{-1}$ at $\lambda = 880$ nm, which was 2.3 times of the Aethalometer default value of $16.6 \, \text{m}^2 \text{g}^{-1}$. A high correlation ($r = 0.83$) was found between rBC and CO, indicating they were from similar local sources. The derived rBC/CO ratio of $1.54 \, \text{ng m}^{-3} \text{ppbv}^{-1}$ may be representative of the mixed emissions from biofuel burning

15 and diesel trucks in the QHL region.

References

Baumgardner, D., Raga, G., Peralta, O., Rosas, I., Castro, T., Kuhlbusch, T., John, A., and Petzold, A.: Diagnosing black carbon trends in large urban areas using carbon monoxide measurements, J. Geophys. Res., 107, 8342, doi:10.1029/2001JD000626, 2002.
25 Baumgardner, D., Kok, G. L., and Raga, G. B.: On the diurnal variability of particle properties related to light absorbing carbon in Mexico City, Atmos. Chem. Phys., 7, 2517–2526, doi:10.5194/acp-7-2517-2007, 2007.

Bodhaine, B. A.: Aerosol absorption measurements at Barrow, Mauna Loa and the South Pole, J. Geophys. Res., 100, 8967–8975, 1995.

Bond, T. C., Streets, D. G., Yarber, K. F., Nelson, S. M., Woo, J. H., and Klimont, Z.: A technology-based global inventory of black and organic carbon emissions from combustion, J. Geophys. Res., 109, D14203, doi:10.1029/2003JD003697, 2004.

Bond, T. C., Habib, G., and Bergstrom, R. W.: Limitations in the enhancement of visible light absorption due to mixing state, J. Geophys. Res., 111, D20211, doi:10.1029/2006JD007315, 2006.

Cao, J. J., Lee, S. C., Ho, K. F., Zhang, X. Y., Zou, S. C., Fung, K., Chow, J. C., and Watson, J. G.: Characteristics of carbonaceous aerosol in Pearl River Delta Region, China during 2001 winter period, Atmos. Environ., 37, 1451–1460, 2003.

Cao, J. J., Wu, F., Chow, J. C., Lee, S. C., Li, Y., Chen, S. W., An, Z. S., Fung, K. K., Watson, J. G., Zhu, C. S., and Liu, S. X.: Characterization and source apportionment of atmospheric organic and elemental carbon during fall and winter of 2003 in Xi'an, China, Atmos. Chem. Phys., 5, 3127-3137, doi:10.5194/acp-5-3127-2005, 2005.

Cao, J. J., Lee, S. C., Chow, J. C., Watson, J. G., Ho, K., Zhang, R. J., Jin, Z. D., Shen, Z. X., Chen, G. X., and Kang, Y. M.: Spatial and seasonal distributions of carbonaceous aerosols over China, J. Geophys. Res., 112, D22S11, doi:10.1029/2006JD008205, 2007.

Cao, J. J., Xu, B. Q., He, J. Q., Liu, X. Q., Han, Y. M., Wang, G., and Zhu, C.: Concentrations, seasonal variations, and transport of carbonaceous aerosols at a remote Mountainous region in Western China, Atmos. Environ., 43, 4444–4452, 2009a.

Cao, J. J., Zhu, C. S., Chow, J. C., Watson, J. G., Han, Y. M., Wang, G., Shen, Z., and An, Z. S.: Black carbon relationships with emissions and meteorology in Xi'an, China, Atmos. Res., 94, 194–202, 2009b.

Cao, J. J., Tie, X. X., Xu, B. Q., Zhao, Z. Z., Zhu, C. S., Li, G. H., and Liu, S. X.: Measuring and modeling black carbon (BC) contamination in the SE Tibetan Plateau, J. Atmos. Chem., 67, 45–60, 2010.

Chameides, W. L., Yu, H., Liu, S., Bergin, M., Zhou, X., Mearns, L., Wang, G., Kiang, C., Saylor, R., and Luo, C.: Case study of the effects of atmospheric aerosols and regional haze on agriculture: an opportunity to enhance crop yields in China through emission controls?, P. Natl. Acad. Sci. USA, 96, 13626–13633, 1999.

Title Page

Abstract | Introduction

Conclusions | References

Tables | Figures

|◄ | ►|

◄ | ►

Back | Close

Full Screen / Esc

Printer-friendly Version

Interactive Discussion

Chung, C. E., Ramanathan, V., Kim, D., and Podgorny, I.: Global anthropogenic aerosol direct forcing derived from satellite and ground-based observations, J. Geophys. Res., 110, D24207, doi:10.1029/2005JD006356, 2005.

Chung, C. E., Ramanathan, V., Carmichael, G., Kulkarni, S., Tang, Y., Adhikary, B., Leung, L. R., and Qian, Y.: Anthropogenic aerosol radiative forcing in Asia derived from regional models with atmospheric and aerosol data assimilation, Atmos. Chem. Phys., 10, 6007–6024, doi:10.5194/acp-10-6007-2010, 2010.

Collaud Coen, M., Weingartner, E., Apituley, A., Ceburnis, D., Fierz-Schmidhauser, R., Flentje, H., Henzing, J. S., Jennings, S. G., Moerman, M., Petzold, A., Schmid, O., and Baltensperger, U.: Minimizing light absorption measurement artifacts of the Aethalometer: evaluation of five correction algorithms, Atmos. Meas. Tech., 3, 457–474, doi:10.5194/amt-3-457-2010, 2010.

Engling, G., Zhang, Y. N., Chan, C. Y., Sang, X. F., Lin, M., Ho, K. F., Li, Y. S., Lin, C. Y., and Lee, J. J.: Characterization and sources of aerosol particles over the Southeastern Tibetan Plateau during the Southeast Asia biomass-burning season, Tellus B, 63, 117–128, 2011.

Forbes, M. S., Raison, R. J., and Skjemstad, J. O.: Formation, transformation and transport of black carbon (charcoal) in terrestrial and aquatic ecosystems, Sci. Total Environ., 370, 190–206, 2006.

Forster, P., Ramanswamy, V., Artaxo, P., Berntsen, T., Betts, R., Fahey, D. W., Haywood, J., Lean, J., Lowe, D. C., Myhre, G., Nganga, J., Prinn, R., Raga, G., Schulz, M., and Dorland, R. V.: Changes in atmospheric constituents and in radiative forcing, in: Climate Change 2007: The Physical Science Basis, Contribution of Working Group I to the Fourth Assessment Report of the Intergovernmental Panel on Climate Change, edited by: Miller, H. L., Cambridge Univ. Press, Cambridge, UK and New York, NY, USA, 129–234, 2007.

Gao, R. S., Schwarz, J. P., Kelly, K. K., Fahey, D. W., Watts, L. A., Thompson, T. L., Spackman, J. R., Slowik, J. G., Cross, E. S., Han, J. H, Davidovits, P., Onasch, T. B., and Worsnop, D. R.: A novel method for estimating light-scattering properties of soot aerosols using a modified single-particle soot photometer, Aerosol Sci. Tech., 41, 125–135, 2007.

Guo, H., Wang, T., Simpson, I., Blake, D., Yu, X., Kwok, Y., and Li, Y.: Source contributions to ambient VOCs and CO at a rural site in Eastern China, Atmos. Environ., 38, 4551–4560, 2004.

Han, Y. M., Han, Z. W., Cao, J. J., Chow, J. C., Watson, J. G., An, Z. S., Liu, S. X., and Zhang, R. J.: Distribution and origin of carbonaceous aerosol over a rural high-mountain

Title Page

Abstract	Introduction
Conclusions	References
Tables	Figures

◀◀ ▶▶

◀ ▶

Back Close

Full Screen / Esc

Printer-friendly Version

Interactive Discussion

lake area, Northern China and its transport significance, Atmos. Environ., 42, 2405–2414, 2008.

Hansen, A., Rosen, H., and Novakov, T.: The aethalometer – an instrument for the real-time measurement of optical absorption by aerosol particles, Sci. Total Environ., 36, 191–196, 1984.

Huang, X. F., Gao, R. S., Schwarz, J. P., He, L. Y., Fahey, D. W., Watts, L. A., McComiskey, A., Cooper, O. R., Sun, T. L., and Zeng, L. W.: Black carbon measurements in the Pearl River Delta region of China, J. Geophys. Res., 116, D12208, doi:10.1029/2010JD014933, 2011.

Huang, X. F., Sun, T. L., Zeng, L. W., Yu, G. H., and Luan, S. J.: Black carbon aerosol characterization in a coastal city in South China using a single particle soot photometer, Atmos. Environ., 51, 21–28, 2012.

IPCC: Summary for Policymakers, Climate Change 2007: The Physical Science Basis. Contribution of Working Group I to Fourth Assessment report of the Intergoverment Panel on Climate Change, Cambridge University Press, Cambridge, New York, 2007.

Jacobson, M. Z.: Climate response of fossil fuel and biofuel soot, accounting for soot's feedback to snow and sea ice albedo and emissivity, J. Geophys. Res., 109, D21201, doi:10.1029/2004JD004945, 2004.

Jacobson, M. Z.: Effects of externally-through-internally-mixed soot inclusions within clouds and precipitation on global climate, J. Phys. Chem. A, 110, 6860–6873, 2006.

Jeong, C. H., Hopke, P. K., Kim, E., and Lee, D. W.: The comparison between thermal-optical transmittance elemental carbon and Aethalometer black carbon measured at multiple monitoring sites, Atmos. Environ., 38, 5193–5204, 2004.

Jin, Z. D., You, C. F., Yu, T. L., and Wang, B. S.: Sources and flux of trace elements in river water collected from the Lake Qinghai catchment, NE Tibetan Plateau, Appl. Geochem., 25, 1536–1546, 2010.

Kang, S., Li, C., Wang, F., Zhang, Q., and Cong, Z.: Total suspended particulate matter and toxic elements indoors during cooking with yak dung, Atmos. Environ., 43, 4243–4246, 2009.

Kondo, Y., Komazaki, Y., Miyazaki, Y., Moteki, N., Takegawa, N., Kodama, D., Deguchi, S., Nogami, M., Fukuda, M., and Miyakawa, T.: Temporal variations of elemental carbon in Tokyo, J. Geophys. Res., 111, D12205, doi:10.1029/2005JD006257, 2006.

Kondo, Y., Matsui, H., Moteki, N., Sahu, L., Takegawa, N., Kajino, M., Zhao, Y., Cubison, M., Jimenez, J., Vay, S., Diskin, G. S., Anderson, B., Wisthaler, A., Mikoviny, T., Fuelberg, H. E., Blake, D. R., Huey, G., Weinheimer, A. J., Knapp, D. J., and Brune, W. H.: Emissions of black

Single particle characterization of black carbon aerosol

Q. Y. Wang et al.

carbon, organic, and inorganic aerosols from biomass burning in North America and Asia in 2008, J. Geophys. Res., 116, D08204, doi:10.1029/2010JD015152, 2011.

Lan, Z. J., Huang, X. F., He, L. Y., Hu, M., Xue, L., Sun, T. L., Hu, W. W., Lin, Y., Zhang, Y. H.: Comparison of measurement results of several online carbonaceous aerosol monitoring techniques, Acta Scientiarum Naturalium Universitatis Pekinensis, 47, 159–165, 2011 (in Chinese).

Li, C., Kang, S., Chen, P., Zhang, Q., Guo, J., Mi, J., Basang, P., Luosang, Q., and Smith, K. R.: Personal $PM_{2.5}$ and indoor CO in nomadic tents using open and chimney biomass stoves on the Tibetan Plateau, Atmos. Environ., 59, 207–213, 2012.

Liousse, C., Cachier, H., and Jennings, S.: Optical and thermal measurements of black carbon aerosol content in different environments: variation of the specific attenuation cross-section, sigma (σ), Atmos. Environ., 27, 1203–1211, 1993.

Lister, G. S., Kelts, K., Zao, C. K., Yu, J. Q., and Niessen, F.: Lake Qinghai, China: closed-basin like levels and the oxygen isotope record for ostracoda since the latest Pleistocene, Palaeogeogr. Palaeocl., 84, 141–162, 1991.

Liu, D., Flynn, M., Gysel, M., Targino, A., Crawford, I., Bower, K., Choularton, T., Jurányi, Z., Steinbacher, M., Hüglin, C., Curtius, J., Kampus, M., Petzold, A., Weingartner, E., Baltensperger, U., and Coe, H.: Single particle characterization of black carbon aerosols at a tropospheric alpine site in Switzerland, Atmos. Chem. Phys., 10, 7389–7407, doi:10.5194/acp-10-7389-2010, 2010.

Ma, J. Z., Tang, J., Li, S. M., and Jacobson, M. Z.: Size distributions of ionic aerosols measured at Waliguan Observatory: implication for nitrate gas-to-particle transfer processes in the free troposphere, J. Geophys. Res., 108, 4541, doi:10.1029/2002JD003356, 2003.

McMeeking, G. R., Hamburger, T., Liu, D., Flynn, M., Morgan, W. T., Northway, M., Highwood, E. J., Krejci, R., Allan, J. D., Minikin, A., and Coe, H.: Black carbon measurements in the boundary layer over Western and Northern Europe, Atmos. Chem. Phys., 10, 9393–9414, doi:10.5194/acp-10-9393-2010, 2010.

Moteki, N., Kondo, Y., Miyazaki, Y., Takegawa, N., Komazaki, Y., Kurata, G., Shirai, T., Blake, D., Miyakawa, T., and Koike, M.: Evolution of mixing state of black carbon particles: aircraft measurements over the Western Pacific in March 2004, Geophys. Res. Lett., 34, L11803, doi:10.1029/2006GL028943, 2007.

Oshima, N., Koike, M., Zhang, Y., and Kondo, Y.: Aging of black carbon in outflow from anthropogenic sources using a mixing state resolved model: 2. Aerosol optical properties and cloud

Single particle characterization of black carbon aerosol

Q. Y. Wang et al.

Title Page

Abstract	Introduction
Conclusions	References
Tables	Figures

◄ | ►►

◄ | ►

Back | Close

Full Screen / Esc

Printer-friendly Version

Interactive Discussion

condensation nuclei activities, J. Geophys. Res., 114, D18202, doi:10.1029/2008JD011681, 2009.

Oshima, N., Kondo, Y., Moteki, N., Takegawa, N., Koike, M., Kita, K., Matsui, H., Kajino, M., Nakamura, H., and Jung, J.: Wet removal of black carbon in Asian outflow: Aerosol Radiative Forcing in East Asia (A-FORCE) aircraft campaign, J. Geophys. Res., 117, D03204, doi:10.1029/2011JD016552, 2012.

Petters, M. D., Prenni, A. J., Kreidenweis, S. M., DeMott, P. J., Matsunaga, A., Lim, Y. B., and Ziemann, P. J.: Chemical aging and the hydrophobic-to-hydrophilic conversion of carbonaceous aerosol, J. Geophys. Res., 33, L24806, doi:10.1029/2006GL027249, 2006.

Ping, X., Jiang, Z., and Li, C.: Status and future perspectives of energy consumption and its ecological impacts in the Qinghai–Tibet region, Renew. Sust. Energ. Rev., 15, 514–523, 2011.

Pope III, C. A. and Dockery, D. W.: Critical review: health effects of fine particulate air pollution: Lines that connect, J. Air Waste Manage., 56, 709–742, 2006.

Schnaiter, M., Linke, C., Möhler, O., Naumann, K. H., Saathoff, H., Wagner, R., Schurath, U., and Wehner, B.: Absorption amplification of black carbon internally mixed with secondary organic aerosol, J. Geophys. Res., 110, D19204, doi:10.1029/2005JD006046, 2005.

Schwarz, J. P., Gao, R. S., Fahey, D. W., Thomson, D. S., Watts, L. A., Wilson, J. C., Reeves, J. M., Darbeheshti, M., Baumgardner, D. G., Kok, G. L., Chung, S. H., Schulz, M., Hendricks, J., Lauer, A., Kärcher, B., Slowik, J. G., Rosenlof, K. H., Thompson, T. L., Langford, A. O., Loewenstein, M., and Aikin, K. C.: Single-particle measurements of midlatitude black carbon and light-scattering aerosols from the boundary layer to the lower stratosphere, J. Geophys. Res., 111, D16207, doi:10.1029/2006JD007076, 2006.

Schwarz, J. P., Gao, R. S., Spackman, J. R., Watts, L. A., Thomson, D. S., Fahey, D. W., Ryerson, T. B., Peischl, J., Holloway, J. S., Trainer, M., Frost, G. J., Baynard, T., Lack, D. A., de Gouw, J. A., Warneke, C., and Negro, A. D.: Measurement of the mixing state, mass, and optical size of individual black carbon particles in urban and biomass burning emissions, Geophys. Res. Lett., 35, L13810, doi:10.1029/2008GL033968, 2008.

Sharma, S., Brook, J., Cachier, H., Chow, J., Gaudenzi, A., and Lu, G.: Light absorption and thermal measurements of black carbon in different regions of Canada, J. Geophys. Res., 107, 4771, doi:10.1029/2002JD002496, 2002.

Title Page

Abstract | Introduction

Conclusions | References

Tables | Figures

◀◀ | ▶▶

◀ | ▶

Back | Close

Full Screen / Esc

Printer-friendly Version

Interactive Discussion

Shiraiwa, M., Kondo, Y., Moteki, N., Takegawa, N., Sahu, L., Takami, A., Hatakeyama, S., Yone-mura, S., and Blake, D.: Radiative impact of mixing state of black carbon aerosol in Asian outflow, J. Geophys. Res., 113, D24210, doi:10.1029/2008JD010546, 2008.

Slowik, J. G., Cross, E. S., Han, J. H., Davidovits, P., Onasch, T. B., Jayne, J. T., Williams, L. R., Canagaratna, M. R., Worsnop, D. R., and Chakrabarty, R. K.: An inter-comparison of instruments measuring black carbon content of soot particles, Aerosol Sci. Tech., 41, 295–314, 2007.

Spackman, J., Schwarz, J., Gao, R., Watts, L., Thomson, D., Fahey, D., Holloway, J., de Gouw, J., Trainer, M., and Ryerson, T.: Empirical correlations between black carbon aerosol and carbon monoxide in the lower and middle troposphere, Geophys. Res. Lett., 35, L19816, doi:10.1029/2008GL035237, 2008.

Subramanian, R., Khlystov, A. Y., and Robinson, A. L.: Effect of peak inert-mode temperature on elemental carbon measured using thermal-optical analysis, Aerosol Sci. Tech., 40, 763–780, 2006.

Subramanian, R., Roden, C. A., Boparai, P., and Bond, T. C.: Yellow beads and missing particles: trouble ahead for filter-based absorption measurements, Aerosol Sci. Tech., 41, 630–637, 2007.

Subramanian, R., Kok, G. L., Baumgardner, D., Clarke, A., Shinozuka, Y., Campos, T. L., Heizer, C. G., Stephens, B. B., de Foy, B., Voss, P. B., and Zaveri, R. A.: Black carbon over Mexico: the effect of atmospheric transport on mixing state, mass absorption cross-section, and BC/CO ratios, Atmos. Chem. Phys., 10, 219–237, doi:10.5194/acp-10-219-2010, 2010.

Tripathi, S. N., Dey, S., Tare, V., and Satheesh, S. K.: Aerosol black carbon radiative forcing at an industrial city in Northern India, Geophys. Res. Lett., 32, L08802, doi:10.1029/2005GL022515, 2005.

Tu, J., Xia, Z.-G., Wang, H., and Li, W.: Temporal variations in surface ozone and its precursors and meteorological effects at an urban site in China, Atmos. Res., 85, 310–337, 2007.

Warneke, C., Bahreini, R., Brioude, J., Brock, C., De Gouw, J., Fahey, D., Froyd, K., Holloway, J., Middlebrook, A., and Miller, L.: Biomass burning in Siberia and Kazakhstan as an important source for haze over the Alaskan Arctic in April 2008, Geophys. Res. Lett., 36, L02813, doi:10.1029/2008GL036194, 2009.

Watson, J. G., Chow, J. C., and Chen, L. W. A.: Summary of organic and elemental carbon/black carbon analysis methods and intercomparisons, Aerosol Air Qual. Res., 5, 65–102, 2005.

Single particle characterization of black carbon aerosol

Q. Y. Wang et al.

Title Page

Abstract	Introduction
Conclusions	References
Tables	Figures

◄ | ►◄

◄ | ►

Back | Close

Full Screen / Esc

Printer-friendly Version

Interactive Discussion

Wild, M., Ohmura, A., and Makowski, K.: Impact of global dimming and brightening on global warming, Geophys. Res. Lett., 34, L04702, doi:10.1029/2006GL028031, 2007.

Wolff, E. W. and Cachier, H.: Concentrations and seasonal cycle of black carbon in aerosol at a coastal Antarctic station, J. Geophys. Res., 103, 11033–11041, 1998.

Xu, H., Ai, L., Tan, L., and An, Z.: Stable isotopes in bulk carbonates and organic matter in recent sediments of Lake Qinghai and their climatic implications, Chem. Geol., 235, 262–275, 2006.

Zhang, X. Y., Wang, Y. Q., Zhang, X. C., Guo, W., Niu, T., Gong, S. L., Yin, Y., Zhao, P., Jin, J. L., and Yu, M.: Aerosol monitoring at multiple locations in China: contributions of EC and dust to aerosol light absorption, Tellus B, 60, 647–656, 2008.

Title Page

Abstract | Introduction

Conclusions | References

Tables | Figures

◄ | ►

◄ | ►

Back | Close

Full Screen / Esc

Printer-friendly Version

Interactive Discussion

Table 1. Summary of rBC concentrations, CO mixing ratio, and number fraction of coated rBC during the sampling period.

Parameter	Average	S.D.	Maximum	Minimum
rBC (μg STP-m^{-3})	0.36	0.27	1.56	0.05
CO (ppbv)	219.7	114.6	634.2	33.7
Number fraction of coated rBC	36.8	5.3	51.1	19.8

S.D.: standard deviation
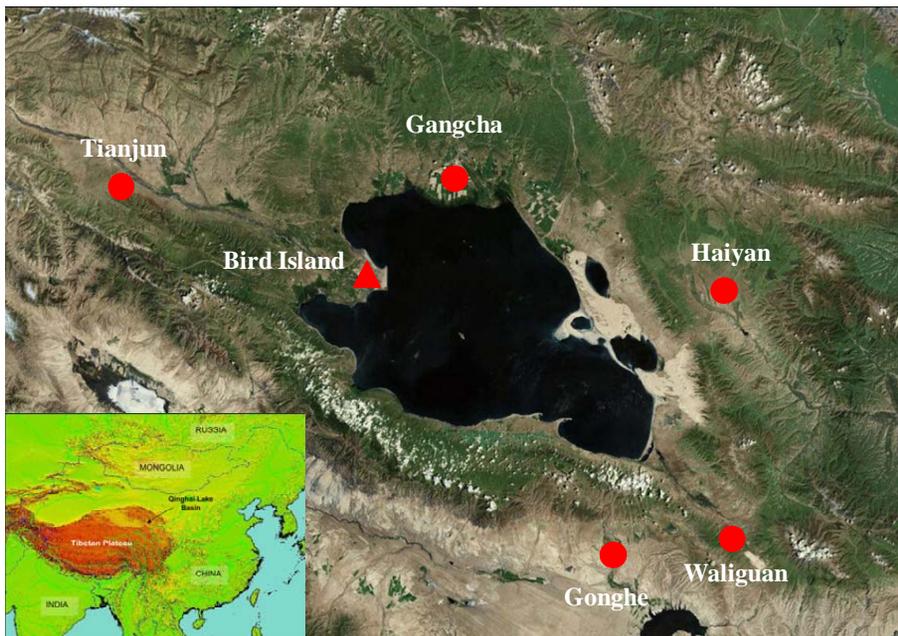
Fig. 1. The map of the sampling site at Qinghai Lake and surrounding regions.
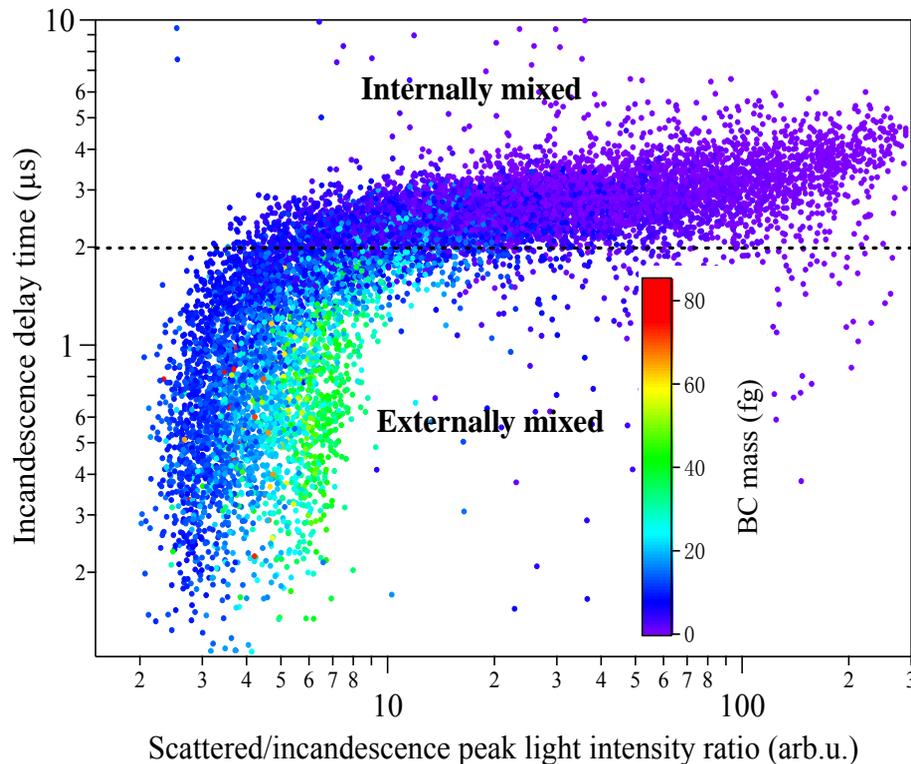
Fig. 2. Correlation plot of SP2 signal diagnostics obtained from individual incandescing particles detected in ambient air. Particles with an incandescence delay time greater than 2 µs are considered to have a substantial coating and, hence, are internally mixed. The color bar shows the mass of individual particles.

Full Screen / Esc

Printer-friendly Version

Interactive Discussion
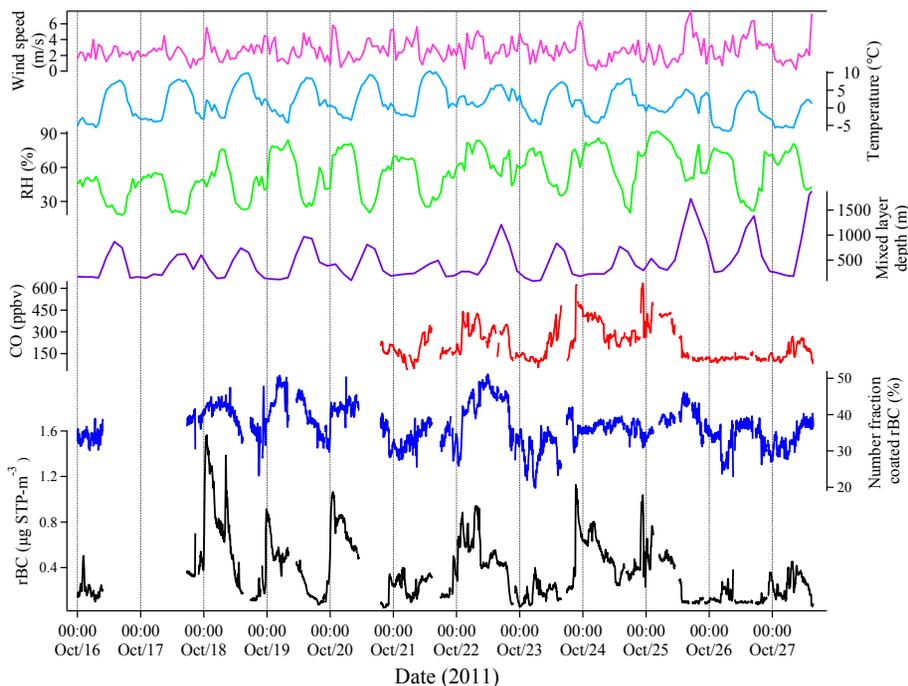
Fig. 3. Time series of 5-min averaged rBC mass concentration, number fraction of coated rBC particles, and CO mixing ratio, as well as the hourly averaged mixed-layer depth, relative humidity (RH), temperature, and wind speed for the entire experiment.
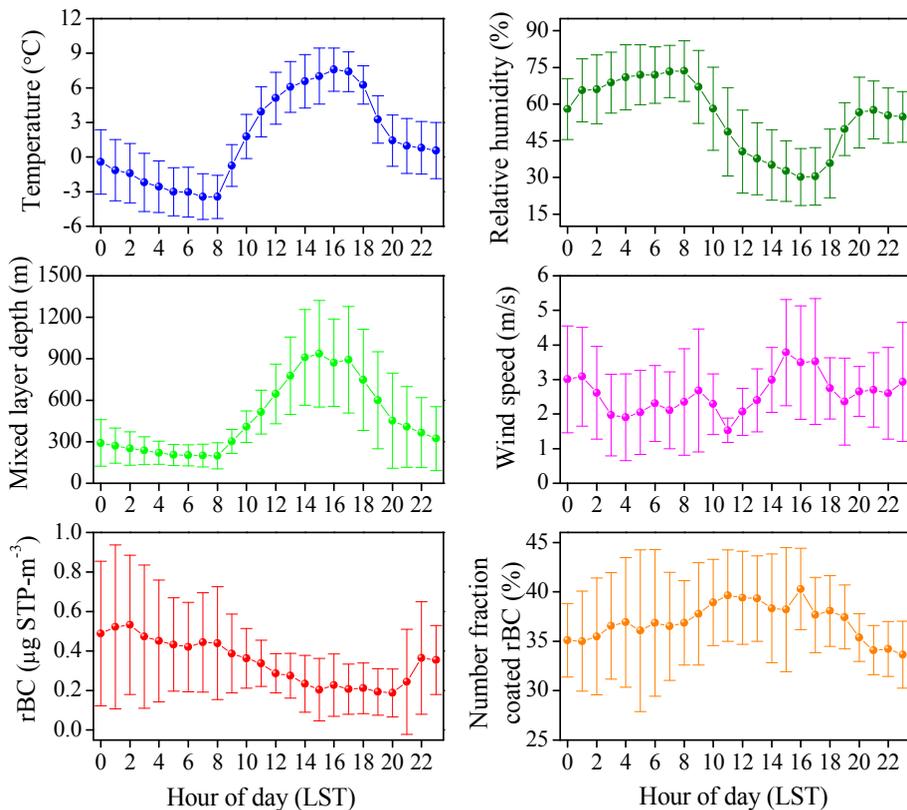
Fig. 4. Diurnal variations of rBC concentration, number fraction of coated rBC particles, mixed-layer depth, wind speed, temperature, and relative humidity. The values are averaged for each hour of the day (error bars represent the standard deviation) for the entire sampling period.
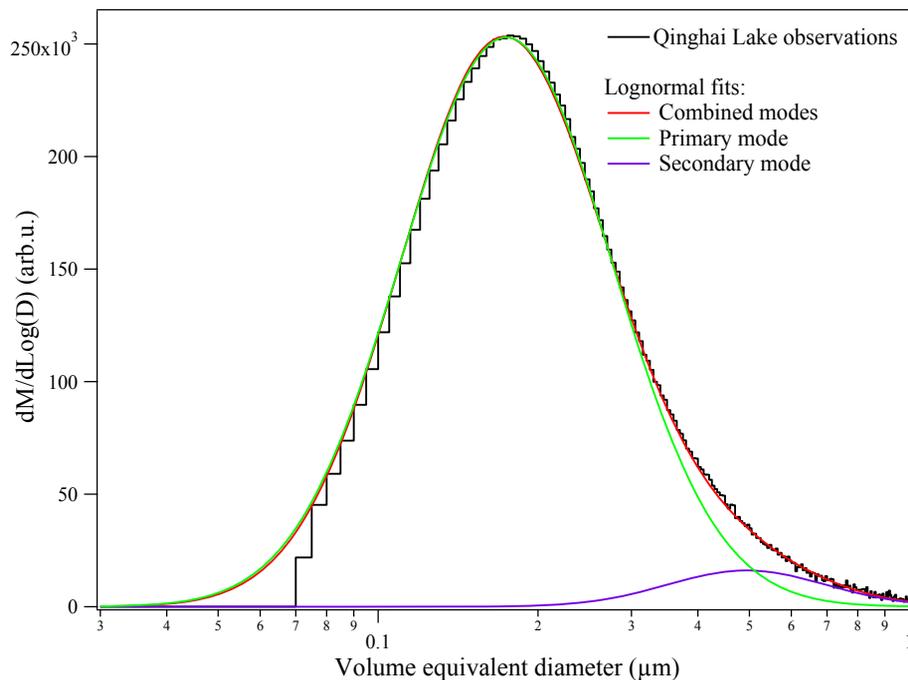
Fig. 5. Size distribution of rBC for the entire sampling period and lognormal fit to the primary and secondary modes and the combined modes. "M" and "D" in vertical label represent rBC mass and diameter, respectively.
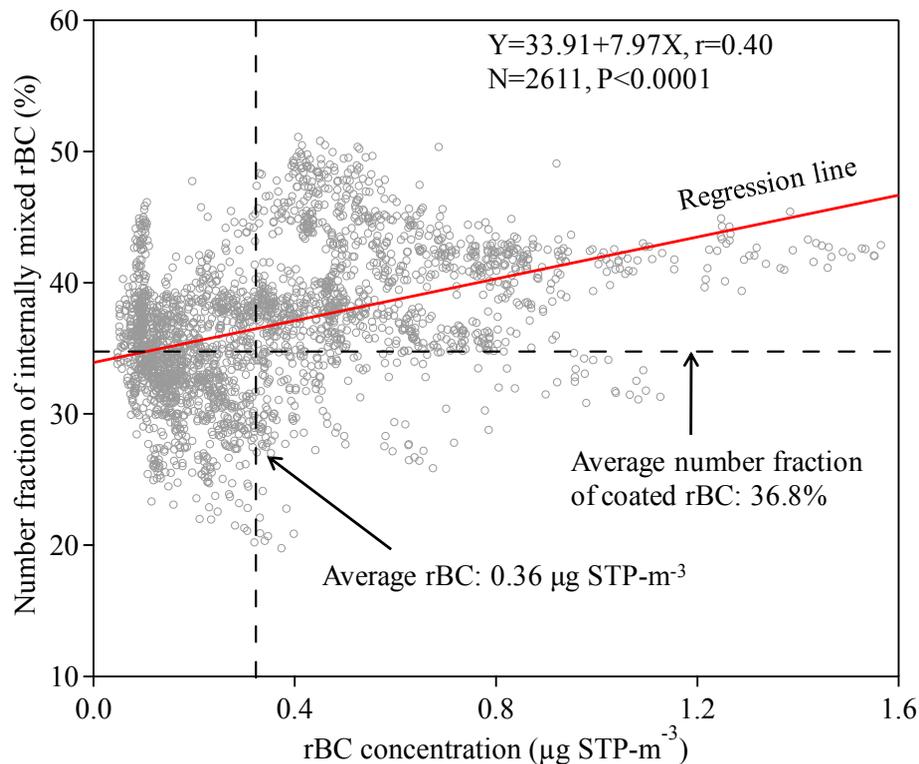
Fig. 6. Scatter plot of rBC concentration versus number fraction of internally mixed rBC during the sampling period. Each data point represents 5-min averaged value. The vertical dashed line is the average rBC concentration and horizon dashed line is the average number fraction of coated rBC. The red line shows the linear fit to all of the data.
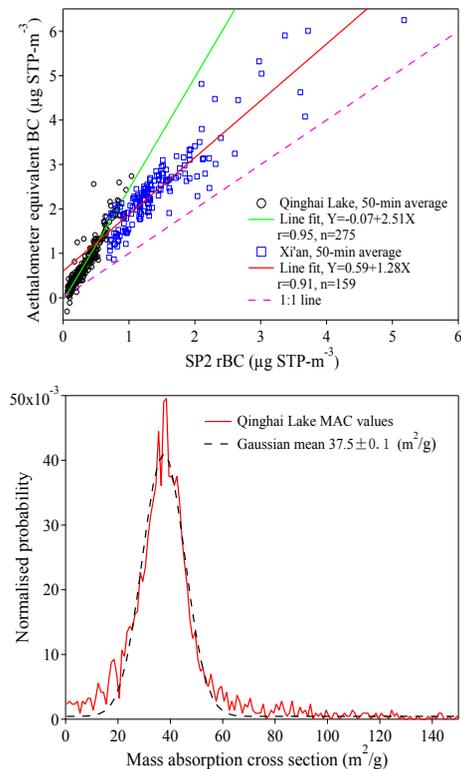
Fig. 7. (a) Correlations between BC concentrations measured by the Aethalometer and rBC concentrations measured with the SP2 from 16 to 27 October 2011 at Qinghai Lake and from 27 June to 3 July 2012 in Xi'an. Each data point is a 50-min average. The solid lines show the linear fits to the corresponding data. **(b)** Probability distribution of derived MAC values during the sampling period in Qinghai Lake (red line) and a Gaussian fit to the data (dashed line) with the mean value indicated.

BC= (1.54±0.05)×CO-(25.07±12.10)
r=0.83 (n=1761, P<0.0001)
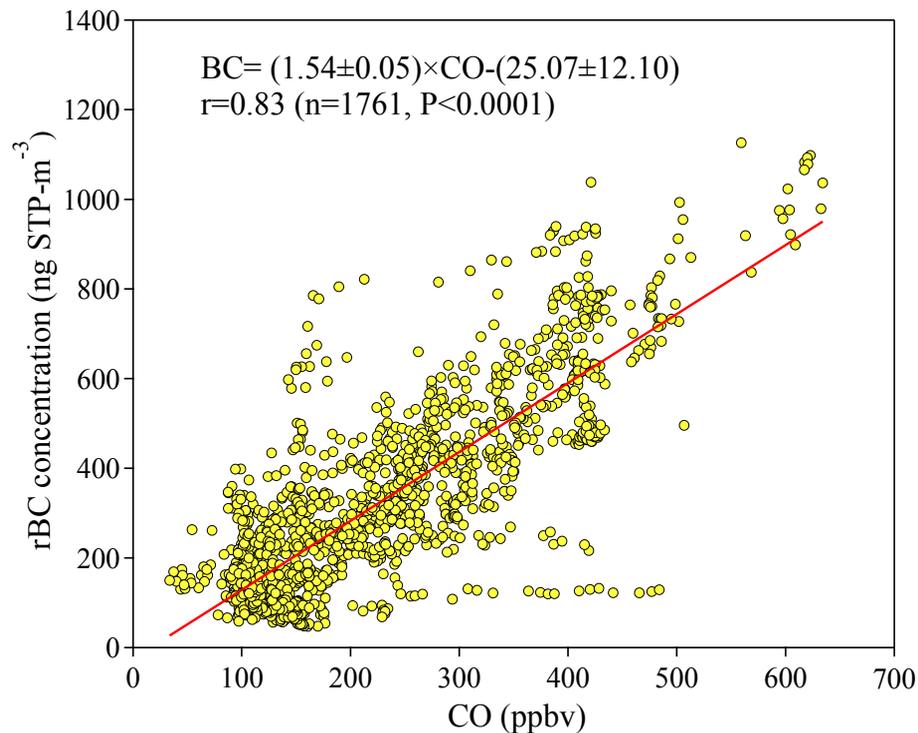
Fig. 8. Scatter plot of rBC concentration versus CO during the sampling period. Each data point represents 5-min average. The linear fit to all of the data is shown with the red line.

Title Page

Abstract | Introduction

Conclusions | References

Tables | Figures

|◀ | ▶|

◀ | ▶

Back | Close

Full Screen / Esc

Printer-friendly Version

Interactive Discussion